Formation of Polymer Microrods in Shear Flow by Emulsification − Solvent Attrition Mechanism

Rossitza G. Alargova,[†,‡] Vesselin N. Paunov,[§] and Orlin D. Velev*[,†]

Department of Chemical and Biomolecular Engineering, North Carolina State University, Raleigh, North Carolina 27695-7905, and Surfactant & Colloid Group, Department of Chemistry, University of Hull, Hull HU6 7RX, United Kingdom

Received July 6, 2005. In Final Form: October 5, 2005

Rodlike polymer particles could have interesting properties and could find many practical applications; however, few methods for the production of such particles are available. We report a systematic study of a droplet shearing process for the formation of polymer rods with micrometer or submicrometer diameter and a length of up to tens of micrometers. The process is based on emulsification of a polymer solution under shear, combined with solvent attrition in the surrounding organic medium. The droplets deform and elongate into cylinders, which solidify when the solvent transfers to the dispersion medium. Stopped flow experiments allow distinguishing all stages of the mechanism. The results are interpreted on the basis of the theory of droplet elongation and breakup under shear. The effects of the viscosity ratio and shear stress are matched against the theoretical expectations. The method is simple, efficient, and scalable, and we demonstrate how it can be controlled and modified. The experimental parameters that allow varying the rod size and aspect ratio include shear rate, medium viscosity, and polymer concentration. Examples of the specific properties of the polymer rods, including self-organization, alignment in external fields and in fluid flows, and stabilization of bubbles, droplets, and capsules, are presented.

1. Introduction

The assembly of colloidal particles is one of the major routes for making nano- and microstructured materials.[1,2] The useful features of the materials synthesized are determined by the properties of the colloidal building blocks used in the assembly. The particle size and shape can be distinguished as the most important parameters in achieving functionality in one, two, or three dimensions. The use of particles of anisotropic shape is of significant interest since it allows fabrication of structures with special symmetries and degree of packing and/or anisotropic properties. The entropic effects during the organization of rodlike particles into colloidal liquid crystals have been studied intensively for decades[3,4] but mostly theoretically or by using biological particles such as viruses.[5,6] A few studies utilizing other rodlike particles have demonstrated the potential of the anisotropic colloids in preparing new liquid-crystalline phases.[7−9]

Despite the remarkable recent progress in the synthesis of various nanorods, nanotubes, and nanowires,[10−18] little has been done in the making of rodlike and cylindrical particles on the micrometer scale. Polymeric fibers, tubes, or "pencils" have been prepared by means of a template method.[19−25] The sizes of the particles prepared by templating inside the pores of membranes or zeolites can be well controlled, and the resulting size polydispersity is very low. However, the amount of rods that can be produced by such techniques is limited by the template capacity. The membrane templating procedure is complex and expensive because of the need to make a membrane with highly uniform pores and to destroy it after the particle synthesis is completed. Scaling up for industrial applications remains a problem for most of the processes reported.

We recently introduced a simple method for synthesis of a new class of polymeric microrods based on a liquid−liquid dispersion technique.[26] It is rapid and robust and can be scaled up relatively easily for producing industrial amounts of microrods. The microrods synthesized by this method are of micrometer diameter and up to tens of micrometers in length. These rods could serve as superstabilizers for aqueous foams in the absence of any surfactants,[27] or as emulsifiers[28] and for preparation of new types of capsules.[29]

* To whom correspondence should be addressed. E-mail: odvelev@unity.ncsu.edu. Fax: (919) 515-3465.

† North Carolina State University.

‡ Present address: Vertex Pharmaceutical Inc., 130 Waverly St., Cambridge, MA 02139.

§ University of Hull.

(1) *Colloids and Colloid Assemblies. Synthesis, Modification, Organization, and Utilization of Colloid Particles*; Caruso, F., Ed.; Wiley-VCH: Weinheim, Germany, 2003; Chapters 8−15.

(2) Velev, O. D. In *Handbook of Surfaces and Interfaces of Materials*; Nalwa, H. S., Ed.; Academic Press: San Diego, 2001; Vol. 3, pp 125−163.

(3) Forsyth, P. A.; Marcelja, S., Jr.; Mitchell, D. J.; Ninham, B. W. *Adv. Colloid Interface Sci.* **1978**, *9*, 37.

(4) Vroege, G. J.; Lekkerkerker, H. N. W. *Rep. Prog. Phys.* **1992**, *55*, 1241.

(5) Dogic, Z.; Fraden, S. *Phys. Rev. Lett.* **1997**, *78*, 2417.

(6) Adams, M.; Dogic, Z.; Keller, S. L.; Fraden, S. *Nature* **1998**, *393*, 349.

(7) van Bruggen, M. P. B.; van der Kooij, F. M.; Lekkerkerker, H. N. W. *J. Phys.: Condens. Matter* **1996**, *8*, 9451.

(8) Vliegenthart, G. A.; van Blaaderen, A.; Lekkerkerker, H. N. W. *Faraday Discuss.* **1999**, *112*, 173.

(9) van der Kooij, F. M.; Lekkerkerker, H. N. W. *Phys. Rev. Lett.* **2000**, *84*, 781.

(10) Dresselhaus, M. S.; Dresselhaus, G.; Eklund, P. C. *Science of Fullerenes and Carbon Nanotubes*; Academic Press: San Diego, CA, 1996.

(11) Lieber, C. M. *Solid State Commun.* **1998**, *107*, 607.

(12) Hu, J.; Odom, T. W.; Lieber, C. M. *Acc. Chem. Res.* **1999**, *32*, 435.

(13) Agrait, N.; Yeyati, A. L.; Ruitenbeek, J. M. *Phys. Rep.* **2003**, *377*, 81.

(14) Ding, J.; Liu, G.; Yang, M. *Polymer* **1997**, *38*, 5497.

(15) Yu, Y.; Eisenberg, A. *J. Am. Chem. Soc.* **1997**, *119*, 8383.

(16) Liu, G.; Yan, X.; Duncan, S. *Macromolecules* **2002**, *35*, 9788.

(17) Raez, J.; Tomba, J. P.; Manners, I.; Winnik, M. A. *J. Am. Chem. Soc.* **2003**, *125*, 9546.

(18) Kim, C. U.; Lee, J. M.; Ihm, S. K. *J. Fluorine Chem.* **1999**, *96*, 11.

(19) Martin, C. R. *Chem. Mater.* **1996**, *8*, 1739.

(20) Cepak, V. M.; Martin, C. R. *Chem. Mater.* **1999**, *11*, 1363.

(21) Steinhart, M.; Wendorff, J. H.; Greiner, A.; Wehrspohn, R. B.; Nielsch, K.; Schilling, J.; Choi, J.; Gösele, U. *Science* **2002**, *296*, 1997.

(22) Ai, S.; Lu, G.; He, Q.; Li, J. *J. Am. Chem. Soc.* **2003**, *125*, 11140.

(23) Moon, S. I.; McCarthy, T. J. *Macromolecules* **2003**, ***36***, 4253.

(24) Peng, C.-Y.; Nam, W. J.; Fonash, S. J.; Gu, B.; Sen, A.; Strawhecker, K.; Natarajan, S.; Foley, H. C.; Kim, S. H. *J. Am. Chem. Soc.* **2003**, *125*, 9298.

(25) Fu, M.; Zhu, Y.; Tan, R.; Shi, G. *Adv. Mater.* **2001**, *13*, 1874.

(26) Alargova, R. G.; Bhatt, K. H.; Paunov, V. N.; Velev, O. D. *Adv. Mater.* **2004**, *16*, 1653.

(27) Alargova, R. G.; Warhadpande, D. S.; Paunov, V. N.; Velev, O. D. *Langmuir* **2004**, *20*, 10371.

10.1021/la051825v CCC: $33.50
Published on Web 12/20/2005

The process of rod synthesis involves the shear of polymer solution into an organic liquid, such as glycerol or ethylene glycol, that is miscible with the polymer solvent, but not with the polymer itself. A few concurrent processes take place including emulsification, viscous shear and breakup of the droplets, solvent attrition in the medium, solidification, and potential subsequent breakup. Here we focus on the colloidal basics of the processes leading to microrod formation. The experiments and analysis reveal the most important parameters influencing the rod formation and their role for determining the quality and the sizes of the formed particles. We demonstrate how the size and shape of the rods can be controlled, and how their properties can be modified to yield colloidal precursors for novel materials and products.

2. Experimental Section

2.1. Materials. Photocurable epoxy resin SU-8 (widely used as a negative resist for photolithography) was purchased from MicroChem, Massachusetts, as a 63 wt % solution (SU-8 25) in γ-butyrolactone (GBL). The resin was used as received or diluted further with GBL. Analytical grade glycerin and its mixtures with analytical grade ethylene glycol, ethanol, and methanol (all from Fisher Scientific, Pennsylvania) and 2-propanol (LabChem, Inc., Pennsylvania) were used without further purification as dispersion media. These solvents are at least partially miscible with the primary SU-8 solvent, GBL, which is a necessary condition for the microrod synthesis. Polystyrene granules of molecular weight 225000 were obtained from Sigma-Aldrich, Missouri. BioMag supermagnetic spheres (Bangs Labs, Inc., Indiana) with a mean diameter of 1.8 μm, received as a 5.4 wt % suspension in water, were used in the fabrication of magnetic microrods. The magnetic particles are comprised of an about 90 wt % iron oxide core, covered by a silane layer. Dry powder from silica spheres of 1 μm average diameter was also provided by Bangs Laboratories.

2.2. Polymer Microrod Preparation. The polymer (SU-8) rodlike particles were synthesized using variations of the liquid−liquid dispersion technique described earlier.[26] The shear mixing of the phases was performed by a Servodyne electronic mixer (Cole-Parmer, Illinois) providing a high speed of stirring (150−6000 rpm) at low torque. It was equipped with a high-shear impeller of diameter 50.8 mm (Lightin A-320, Cole-Parmer), inserted into a beaker of inner diameter 62.2 mm. The experimental protocol typically included the following stages: First, the container was filled with 50 mL of dispersion medium comprised of pure glycerin, or solvent mixtures. Second, the impeller was introduced into the medium and the homogenizer was started. The shear flow develops fully in 5−10 s. Third, 0.1−0.5 mL of the polymer solution (30−63 wt % SU-8 in GBL or other solvent) was injected directly into the gap between the impeller and the vessel, thus being immediately subjected to a viscous shearing by the mixer. The system was stirred for 10 min or for varying time in the case of stopped flow experiments.

The process resulted in a suspension of polymer microrods in the organic medium. The polymer particles were cross-linked by exposure to 365 nm UV light (BL-100A UV lamp, Blak-Ray, California) for 15 min. The separation and transfer of the synthesized rods into another dispersion medium was done either by centrifugation or by filtration. To prepare rod dispersion in water, the initial dispersion of rods in glycerin or its mixtures was diluted twice with deionized (DI) water (from a Millipore RiOs 16 RO unit), and filtered through a 0.45 mm Durapore membrane (Millipore, Massachusetts) to separate the particles. The rods collected on the membrane were repeatedly washed with DI water to remove traces of organic solvents and then suspended in deionized water to produce a dispersion of a given solid content. Dispersions of SU-8 rods in dodecane and 2-propanol were prepared by similar procedures.

Preparation of magnetic SU-8 microrods was carried out following the same procedure as for pure SU-8 rods. The superparamagnetic particles were first separated from the water phase in a magnetic field, and the supernatant was removed and replaced by ethanol. This procedure was repeated three times, after which the BioMag particles were dried for the complete removal of the ethanol, and dispersed in GBL. This particle dispersion was then mixed with SU-8 solution in GBL (63 wt %) to yield a mixture containing 1.55 wt % magnetic particles and 48.6 wt % SU-8. The particle/SU-8 mixture was used as the initial polymer solution in the procedure described above.

The synthesized particles were characterized by using optical microscopy (Olympus BX-61 microscope with a DP-70 digital CCD camera) and SEM (JEOL, F6400). The viscosities of the polymer solution and the dispersion media were measured with an Advanced Rheometer AR200 (TA Instruments, Delaware) using concentric cylinders (the inner one rotating with a constant shear rate, the outer one immobile) with a gap of 500 μm between them.

3. Emulsion Drops in a Controlled Shear Flow

The emulsification of the initial polymer solution and the consecutive deformation of the drops in the shear flow are critical stages of the rod formation process. Here we summarize the parameters used to describe the flow and the basics of response of emulsion drops to shear that were used to interpret the data.

The high viscosity of the continuous phases and the use of a shear impeller allows us to assume that the flow in our device is predominantly simple shear, similar to the one induced in the thin gap between two concentric cylinders. The simple shear flow is characterized by the shear rate, G, and shear stress, τ, given by the following equations:[30]

$$G = \frac{\mathrm{d}v}{\mathrm{d}x} \approx \frac{\text{linear velocity}}{\text{gap size}} \tag{1}$$

and

$$\tau = \mu_0 G \tag{2}$$

where μ_0 is the viscosity of the dispersion medium. High values of τ are achieved by increasing G and/or μ_0. This equation is strictly applicable only to mixing with concentric cylinder or other specialized devices, but provides a reasonable basis for characterization of shear flows on scales comparable to the size of the particles synthesized here.

Starting with the work of Taylor,[31] many experimental and theoretical studies in the literature have considered how an emulsion drop deforms and bursts into smaller drops when subjected to a shear stress in quasi-static conditions. The droplet breakup occurs when the dimensionless capillary number, Ca, reaches a certain critical value.[30,32−37] The capillary number evaluates the ability of the interfacial tension to counteract the deformation induced by the shear stress. It is defined as a ratio between the shear stress and the Laplace pressure:

$$\mathrm{Ca} = \mu_0 G a/\gamma \tag{3}$$

where a is the radius of the drop before the deformation and γ

(28) Noble, P. F.; Alargova, R. G.; Velev, O. D.; Paunov, V. N. *J. Mater. Chem*., submitted for publication.
(29) Noble, P. F.; Cayre, O. J.; Alargova, R. G.; Velev, O. D.; Paunov, V. N. *J. Am. Chem. Soc.* **2004**, *126*, 8092.
(30) Van de Ven, T. G. M. *Colloidal Hydrodynamics*; Academic Press: San Diego, CA, 1989; Chapter 3.
(31) Taylor, G. I. *Proc. R. Soc. London, A* **1934**, *146*, 501.
(32) Rallison, J. M. *Annu. Rev. Fluid Mech.* **1984**, *16*, 45.
(33) Stone, H. A. *Annu. Rev. Fluid. Mech.* **1994**, *26*, 65
(34) Mason, T. G.; Bibette, J. *Phys. Rev. Lett.* **1996**, *77*, 3481.
(35) Li, J.; Renardy, Y. Y.; Renardy, M. *Phys. Fluids* **2000**, *12*, 269.
(36) Sugiura, S.; Nakajima, M.; Kumazawa, N.; Iwamoto, S.; Seki, M. *J. Phys. Chem.* **2002**, *106*, 9405.
(37) Schmitt, V.; Leal-Calderon, F.; Bibette, J. *Top. Curr. Chem.* **2003**, *227*, 195.

is the interfacial tension. The droplets are deformed when the viscous stress of the external phase, $\mu_0 G$, overcomes the Laplace pressure created by the interfacial tension, γ/a. Deformation and breakup will occur more easily when the droplets are large, or when the interfacial tension is low.

The critical values of Ca for droplet breakup depend on another dimensionless parameter, the viscosity ratio $p = \mu_1/\mu_0$ (μ_1 is the viscosity of the dispersed phase, SU-8 solution), and usually are on the order of unity.[32−37] Droplets with much larger capillary numbers will elongate substantially due to the influence of the viscous shear. They can be regarded as liquid cylinders, susceptible to capillary (Raleigh) instabilities in which the interfacial tension is the driving force for rupturing of the cylinder into spherical drops with less total surface area.[30,37] Depending on the conditions, an elongated drop may break up into two drops of similar volume, or may be stretched even more to form a liquid thread which bursts into a chain of many similar droplets. An elongated droplet may rupture also due to other mechanisms such as tip-streaming and end-pinching. The theoretical description of the droplet behavior in shear flow is complicated, and besides the viscosity ratio, shear stress, and capillary number, it depends on the type and history of the shear flow created.[37]

The shearing geometry and procedures were the same in all experiments, and only G, p, and γ were varied between the experiments. When the viscous deformation is applied in nonstatic conditions (the shear is suddenly applied to the emulsion), a monodisperse fragmentation of the droplets may occur. This phenomenon has been explored recently for production of monodisperse emulsions and particles.[34,37] It is similar to the regime in our study in which the initial polymer solution is injected directly into the dispersion medium at a constant shear rate.

4. Results and Discussion

4.1. Identifying the Major Stages of Microrod Formation. The experimental procedure of polymer rod formation is simple and efficient. The microrods were formed by shearing of an emulsion of a polymer solution into a viscous organic medium. The result was a slightly opalescent milky dispersion. Microscopy observations readily identified that the dispersion was made of microscopic cylinders. Typical optical microscopy and SEM images of the SU-8 microrods are shown in Figure 1a,b. The particles have a uniform cylindrical shape. The process is rapid and typically has a high yield. More than 97% of the SU-8 contained in the initial polymer solution could be converted into rods. The microrods slowly sedimented toward the bottom of the vessel, forming dense phases with a characteristic "liquid-crystal-like" appearance in reflected light. The solid rods could be additionally cross-linked by UV light, which is not a necessary condition for preserving their shape, but makes SU-8 resin extremely inert and insoluble in most common solvents.[38] The cross-linked rods could be separated, washed with water, and eventually resuspended in organic liquids. The rods trapped in thin drying layers of concentrated suspensions in hydrocarbons demonstrated self-organization in small domains resembling in structure nematic liquid crystals (Figure 1c,d).

The shape of the particles implies that they are obtained from liquid droplets elongated under shear flow. The initial stage of emulsification of the polymer solution is probably enhanced by the very low interfacial tension between the polymer solvent and the medium, which are mutually miscible. The mutual miscibility may lead to some degree of self-emulsification due to the mass transfer of GBL through the interface.[39] Because of the spontaneous emulsification and the low interfacial tension, we found out that even slight shear flow leads to formation of elongated particles with a high aspect ratio. It was possible to prepare rodlike SU-8 particles simply using a magnetic stirrer or by handshaking (see the Supporting Information). Mixing of the two phases by means of ultrasound, i.e., without a shear flow, resulted in a formation of small spherical particles instead of rods. The ultrasound experiment thus serves as an indirect confirmation of the importance of the shear flow for the droplet deformation into uniform cylinders.

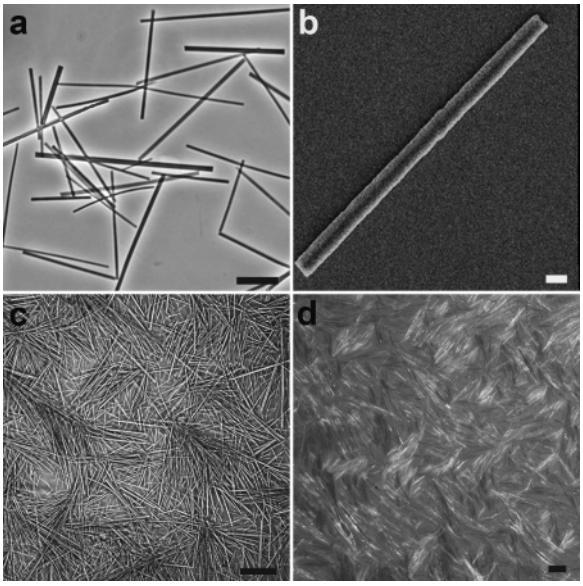

Figure 1. Typical optical microscopy (a, c, d) and SEM (b) micrographs of SU-8 rod suspensions with different solid contents. Image c shows a concentrated dispersion of SU-8 rods in water sedimented on the bottom surface. Image d is a micrograph in crossed polarizers of a layer of SU-8 rods deposited on a glass slide after drying of a drop of rod dispersion in dodecane. The scale bar is 10 μm for (a), 1 μm for (b), and 50 μm for (c) and (d).

The droplets elongated by the shear flow solidify as cylindrical particles with a high aspect ratio due to the rapid transfer of the GBL molecules from the polymer solution into the outside medium, which leads to hardening of the polymer. By performing stopped flow experiments, we found out that formation and solidification of the polymer rods takes between 30 s and a few minutes (2−5 min). Ten minutes was chosen as an optimal time in the experimental protocol. According to our observations, the extra stirring of the already formed drops did not lead to further breaking and deformation. The almost ideal uniform cylindrical shape of the SU-8 rods is clearly seen in SEM images taken at higher magnification (Figure 2a). Strictly speaking, deformation in a cylindrical shear flow could result in some deviation from a circular cross-section, due to the different rates of shear in the horizontal and vertical direction. This is opposed by the capillarity at the different stages of shearing and solvent attrition, and was not observed within the resolution of the SEM instrument used. One additional step in the process causes most of the rods to have flat ends. If every drop deforms and freezes into a single particle, all of the rods would have hemispherical ends. The SEM images, however, show that most of the rods are almost ideal cylinders with flat ends (Figure 2b). The sharp edges imply an additional breaking stage during the rod formation under shear. A relatively small fraction of the rods observed by SEM have hemispherical ends.

(38) Lorenz, H.; Despont, M.; Fahrni, M.; LaBianca, N.; Vettiger, P.; Renaud, P. *J. Micromech. Microeng.* **1997**, *7*, 121.

(39) Evans, D. F.; Wennerström, H. *The Colloidal Domain*; Wiley-VCH: New York, 1999; Chapter 11.

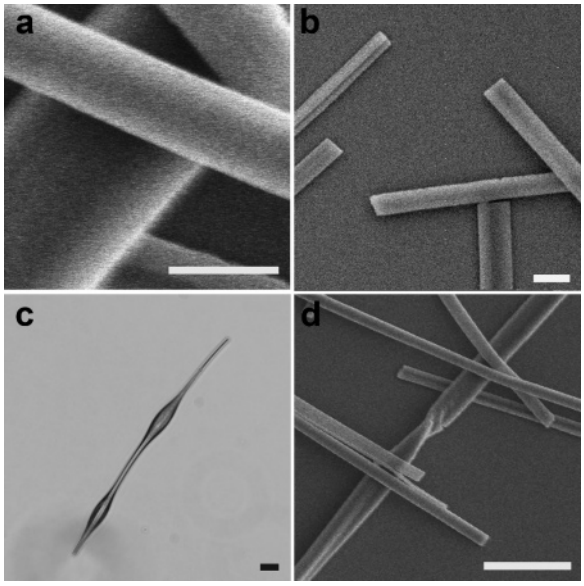

Figure 2. SEM (a, b, d) and optical (c) micrographs of SU-8 rods. Frames a and b demonstrate the uniform cylindrical shape and the sharp edges at the ends. Frame c is an intermediate structure solidified at an early stage of the process, and frame d captures a rod solidified in the process of breaking. The scale bar is 1 μm for (a) and (b) and 10 μm for (c) and (d).

To confirm the proposed mechanism of concurrent droplet elongation and solidification, stopped flow experiments were performed where we abruptly stopped the shear about 30 s after the beginning and let the sample solidify at rest. An example of a particle obtained in such experiments is presented in Figure 2c. This particle shape suggests that, indeed, at an early stage of the process, the polymer solution is in the form of liquid drops which are elongated and exhibit capillary instabilities. Similar formations have been observed with dynamically evolving emulsion droplets subjected to shear stress.[33−37] Hence, during the early stages of the process the polymer solution is emulsified and sheared similarly to common emulsions formed from two immiscible liquid phases. The large droplets are broken into smaller ones, while being sheared by the flow of the surrounding viscous medium.

The last stage of the rod formation process proposed, mechanical breaking of the long fibers into smaller rods with flat ends and sharp edges, was verified experimentally by SEM observations of stopped flow and final samples. Twisted and cracked rods were observed, most probably preserved at an intermittent near-broken stage (Figure 2d). SU-8 is a hard solid resin even before the UV cross-linking, and we were unable to detect a significant degree of breaking of the once-formed solid rod suspensions in shear flows similar to the ones in the emulsifying device. We hypothesize that the breaking occurs before the solvent is fully transferred to the continuous phase, at a stage where SU-8 is beginning to solidify, but is still fragile due to the presence of residual solvent. The important role of the polymer fragility was proved in experiments where we sheared a chloroform solution of high-molecular-weight polystyrene in a glycerin/ethanol mixture (1:1). The process resulted in the formation of a mass of very long uniform polymer fibers resembling the ones made by electrospinning or high-speed extrusion (Figure 3).

The mechanism of microrod formation discussed above is illustrated schematically in Figure 4. We now focus on a more detailed analysis of the initial stages of emulsification and shearing, with the goal of identifying the major parameters that

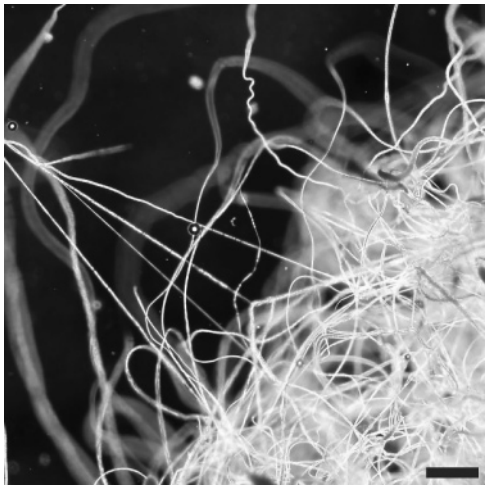

Figure 3. Optical low-magnification micrograph of the result of shearing of a solution of polystyrene of high molecular weight. As the polymer threads are flexible and do not break, the final result is long thin polystyrene fibers instead of rods. The scale bar is 200 μm.

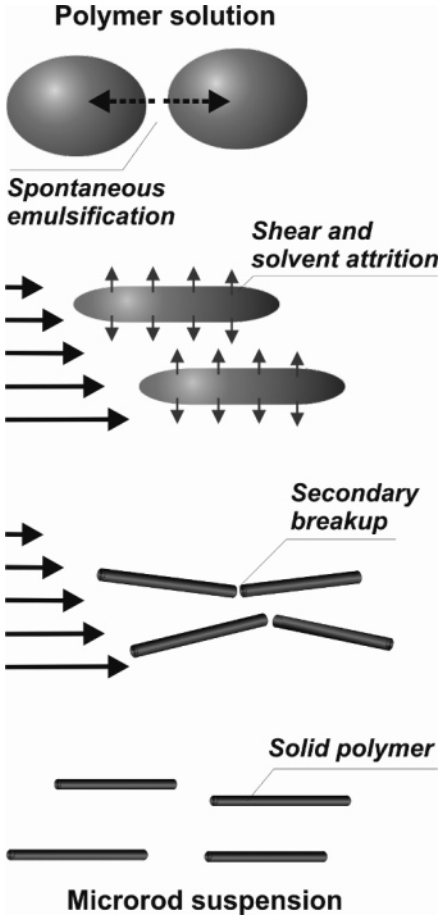

Figure 4. Schematics of the stages of the microrod formation process.

allow control of the process and adjustment of the rod shape and size. The mechanism is complex, as three major processes take place simultaneously during the initial mixing and shearing. These are the emulsification of the initial polymer solution, droplet deformation into cylinders, and the onset of their solidification. Possible coalescence of already formed drops may complicate the process further, but will not be considered here as we have no evidence of this occurring. The micrograph in Figure 2c points out that intermediate stages include bursting of the larger elongated

drops into smaller droplets due to capillary instabilities. Subtle balance between the rates of all these processes determines the properties of the microrods obtained; small variations in the experimental parameters may affect significantly the shapes and the sizes of the synthesized particles. In some cases rodlike particles were not formed at all if a suitable combination of experimental conditions was not met. The sensitivity of the process to key experimental parameters, on the other hand, gives ample freedom to control and modify the types of rods formed. The effects of the major parameters controlling the process, shear stress, τ, critical capillary number, Ca_{cr}, and polymer concentration, were investigated in detail and are presented in the following subsections.

4.2. Effect of the Shear Stress, τ, on the Microrod Characteristic Sizes. The shear stress as defined by eq 2 can be varied either by the shear rate, G, or by the viscosity of the continuous medium, μ_0. We investigated in detail the dependence of the particle sizes and aspect ratio on τ by preparing samples at various G using a 50:50, v/v, mixture of glycerol and ethylene glycol as a dispersion medium. The shear rate was varied from 93 to 930 s^{-1}, changing the applied shear stress by one order of magnitude. The particle sizes were determined by analyzing optical micrographs to obtain the rod length, L, and SEM images to measure the rod diameter, d. The average length was determined by measuring at least 500 particles, while the average diameter was determined by data from 200 particles. Parts a and b of Figure 5 show how both characteristic sizes change as the shear stress imposed increases from 10 to 100 Pa. Both sizes decrease rapidly with the shear stress, but the relative reduction in L is larger. The average length decreases by a factor of about 10, while at the same conditions the average diameter is reduced only by a factor of about 3. Both characteristic rod dimensions begin to level off at values of τ higher than ca. 50 Pa (Figure 5).

The shortest rods were produced at the highest shear stress applied and had an average length of about 16 μm. Theoretically, it may be possible to obtain even shorter rods if the viscous stress imposed is high enough. The geometry and design of our mixing device did not allow us to perform experiments at $\tau > 100$ Pa because of the onset of turbulence, which worsened the quality of the microrods formed and led to irregularly shaped elongated particles. Smaller rods could potentially be synthesized by simultaneous mixing and intensive shearing in a thin gap. We were able to synthesize SU-8 rods with slightly smaller dimensions by shearing inside a rheometer with two concentric cylinders (see the Supporting Information). Achieving much smaller sizes, however, could be difficult as the capillary number decreases with decreasing droplet size and much more mechanical energy will be required for droplet elongation.

The comparison of the data collected at two different SU-8 concentrations in Figure 5a,b shows that decreasing the polymer concentration in the initial solution reduces the sizes of the microrods. This is understandable since less material is present in the dispersed phase while the rest of the conditions are kept almost the same and the emulsification is expected to result in similarly sized droplets. It can be argued that the decrease in the SU-8 concentration would lead to a decrease in the interfacial tension. This change of γ, however, is not expected to be very large, and the interfacial tension of the more concentrated solution is already very low.

The rod aspect ratios for the two SU-8 concentrations studied are plotted in Figure 5c. The L/d ratio decreased with the polymer concentration as discussed above. The largest aspect ratios were achieved at the lowest shear stress. Increasing the shear stress

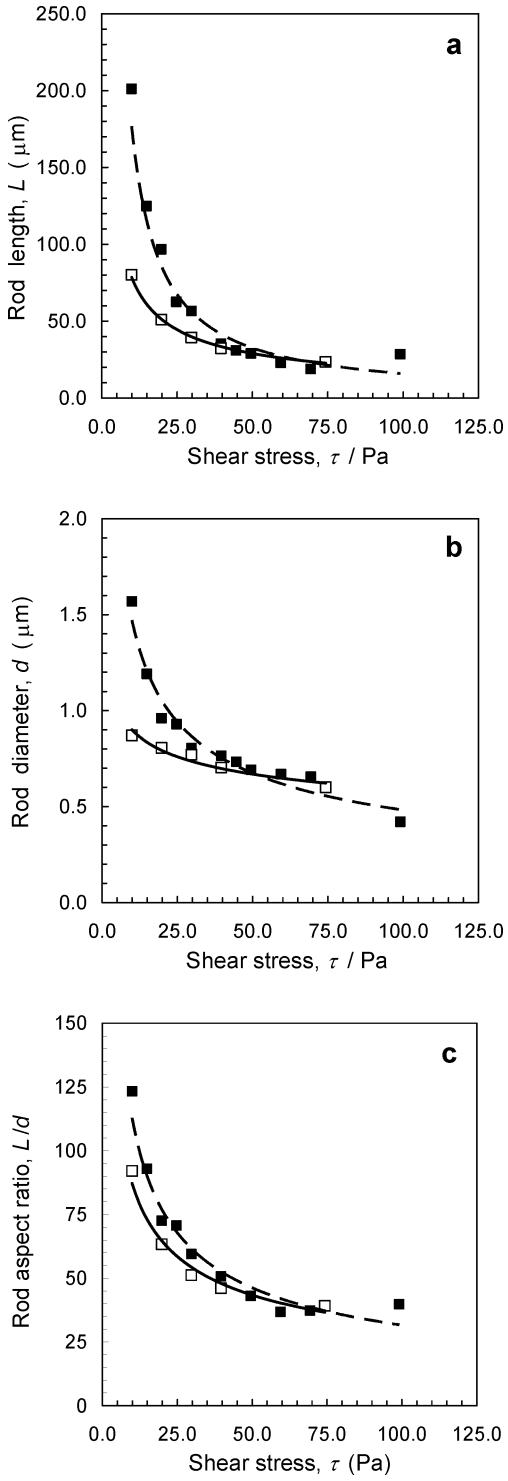

Figure 5. Average (a) length, (b) diameter, and (c) aspect ratio, L/d, of SU-8 rods prepared in 50:50, v/v, glycerol and ethylene glycol as a function of the shear stress. The shear stress is varied through the shear rate. Symbols present data obtained at two different concentrations of SU-8 in the initial polymer solution, 63 wt % (solid symbols) and 48.2 wt % (empty symbols). The lines are a guide to the eye.

decreased not only the average size and aspect ratio of the particles but also their polydispersity. The size distributions measured for two rod samples prepared at low and high shear stress are plotted in Figure 6. The size distributions of both L and d of the particles prepared in the lower τ range (Figure 6a,b) are multimodal. The size distribution of the samples prepared at high τ is much narrower (Figure 6c,d). This is most probably related to the

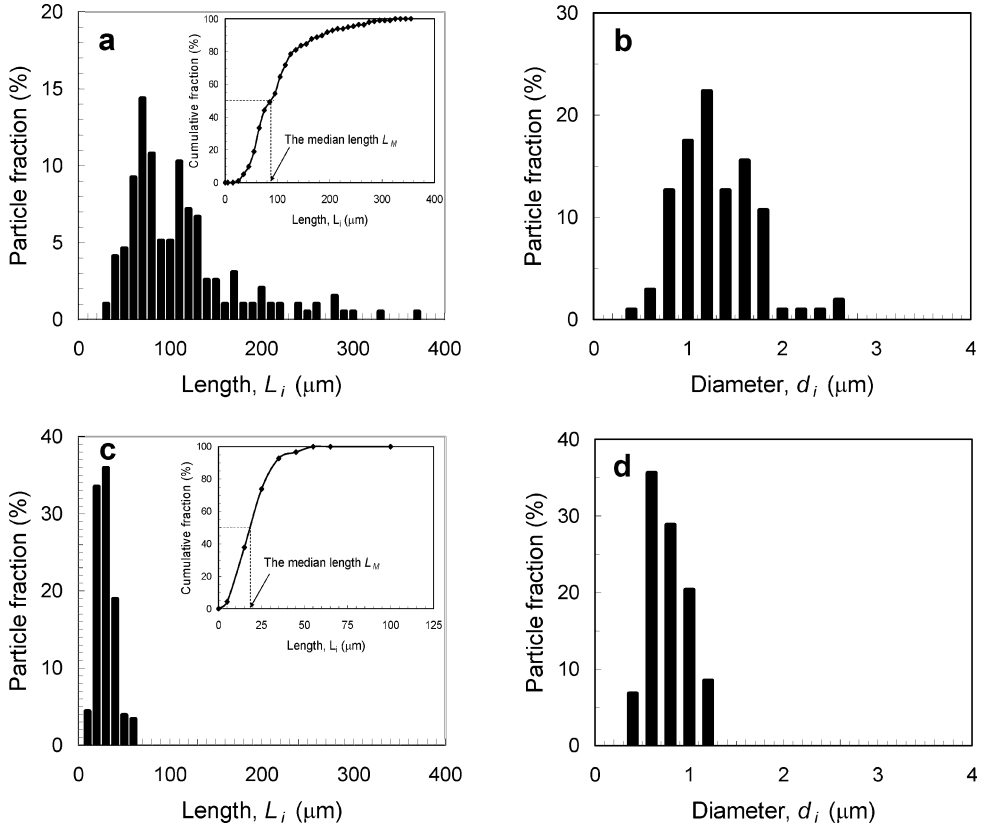

Figure 6. Particle length (a, c) and diameter (b, d) distribution (by number) for rods synthesized at (a, b) a low shear stress of 14.9 Pa and (c, d) a high shear stress of 59.4 Pa. The dispersion medium is glycerol/ethylene glycol at a 1:1 volume ratio.

Table 1. Correlation between the Shear Stress, τ, and the Average Length of SU-8 Microrods, L, for Samples Prepared in Three Dispersion Media of Different Viscosities, μ_0[a]

dispersion medium	μ_0, Pa s	τ, Pa	L, μm
glycerol	1.040	242.5	21.3
75 vol % glycerol, 25 vol % ethanol	0.1491	34.8	53.5
50 vol % glycerol, 50 vol % ethylene glycol	0.1065	24.8	65.6

[a] The shear rate applied was constant at 233.2 s^{-1}. The initial polymer concentration was 63 wt % SU-8 in GBL.

mechanism of emulsification in conditions of controlled shear discussed in section 3. At large shear stress, the values of Ca for the initially formed drops are larger than the critical capillary number. These conditions favor droplet deformation followed by fragmentation into strings of monodisperse smaller drops, and formation of monodisperse microrods. On the contrary, at low τ the capillary numbers for most of the drops formed are small and below the critical capillary number. These elongated drops will solidify into polydisperse rods without bursting.

The applied shear stress could also be altered through the viscosity of the dispersion medium (see eq 2) at a constant shear rate. The corresponding results for a few systems with different medium viscosities are summarized in Table 1. The effect of τ on the microrod sizes was similar to that when τ was varied by means of G. The shortest rods are formed when SU-8 is dispersed in the most viscous medium, glycerol, where the imposed shear rate is highest. The average rod length in this sample is close to the lowest value in Figure 6a. Comparison between rods prepared in a glycerol/ethanol mixture and in a glycerol/ethylene glycol mixture at the same shear stress and SU-8 content show that they have similar sizes. Therefore, the shear stress is established as a factor predictably controlling the rod sizes. This could be a result both of the rapid shearing and fragmentation in smaller droplets and of the subsequent shear-induced breakup of the solidified rods. We believe that the leading effect here is the rapid breakup of the dispersed liquid phase into small elongated droplets before the polymer solvent can diffuse out, similarly to processes for preparing monodisperse emulsions.[34]

4.3. Role of the Capillary Number in the Process of Microrod Formation. The experimental observations point out that the process of polymer rod formation, even though complex, is strongly dependent on the mechanism of emulsion deformation under shear. In section 3 we describe how the mechanism of droplet deformation and fragmentation in a shear flow is related to the capillary number and the viscosity ratio. According to Figure 6, the increase in the shear stress decreases the rod sizes at a constant viscosity ratio. This is analogous to the literature data for the shear-induced formation of monodisperse emulsions,[34,37] which point out that the droplets are broken by capillary instabilities under shear and correlate the size of the droplets formed to the shear rate. If the shear is stopped only 20−30 s after introduction of the SU-8 solution, structures similar to the one in Figure 2c are observed. They resemble the shapes of emulsion drops deformed under shear just before breaking up and point out that capillary instabilities develop on the surface of the cylindrically deformed droplets in the beginning of the process.

To evaluate the role of Ca in our experiments, we analyzed one set of data obtained at a constant viscosity ratio, $p = 33$ and 63 wt % SU-8 (these data are presented by solid symbols in Figure 5). At constant p only drops whose capillary number is around or below a given critical value, Ca_{cr}, will remain intact under shear deformation and lead to formation of rods. Larger drops would rupture after substantial deformation. Therefore, smaller emulsion drops will form at higher values of G and will result in smaller polymer particles after solidification. This

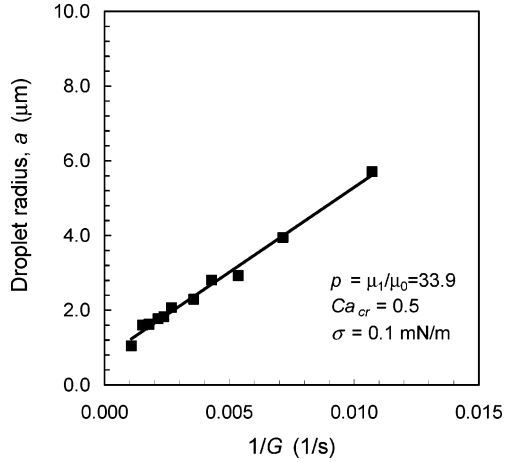

Figure 7. Calculated radius, *a*, of the hypothetical emulsion drops that would correspond to the final rod size measured. According to the expression for the capillary number, the dependence of *a* on the inverse shear rate, G^{-1}, should be a straight line. The correlation coefficient here is 0.99. Assuming $\gamma = 0.1$ mN/m, the critical capillary number calculated from the slope is $Ca_{cr} = 0.5$.

conclusion agrees qualitatively with the data in Figure 5. If we assume that the size of the rods formed is correlated to the size of the droplets broken under shear, i.e., each emulsion drop forms a single rod or the same number of rods, the radius of the original "nondeformed" drops, *a*, will be proportional to the inverse shear rate, 1/*G*, as predicted by eq 3, i.e.

$$a = \frac{Ca_{cr}\gamma}{\mu_0}\frac{1}{G} = A\frac{1}{G} \qquad (4)$$

Here, Ca_{cr} and μ_0 are assumed to be constant and the interfacial tension γ is assumed to vary little during the early stages at which the polymer solution mainly emulsifies. The radius of these hypothetic "precursor" emulsion drops (formed immediately after the emulsion is sheared) was calculated using the average dimensions measured for the synthesized rods and the polymer volume fraction. The experimental plot of *a* vs G^{-1} is fitted well with a straight line (Figure 7). The slope of the line is positive and should be equal to $Ca_{cr}\gamma/\mu_0$, suggesting that the product $Ca_{cr}\gamma$ is constant (as the viscosity of the dispersion medium remains constant).

The fit allows estimating the value of Ca_{cr}. The values of Ca_{cr} cited in the literature for comparatively high values of the viscosity ratio (as in our system) are on the order of unity.[30,32,37] The exact value of γ between partially miscible liquids under the conditions of mass transfer is difficult to measure. We assume that a value of $\gamma \leq 0.1$ mN/m is a reasonable approximation for the interfacial tension of self-emulsifying systems.[39] The corresponding values of the critical capillary number would be $Ca_{cr} \geq 0.5$. Thus, the fit of the data in Figure 7 gives reasonable values, pointing out that while the model based on the kinematics of droplet breakup is simplistic and does not account for all stages of rod formation, it has a certain predictive power regarding the effect of the shear stress on the microrod size.

The straight line in Figure 7, however, has an intercept of 0.75 μm. It implies the existence of a minimal drop size at the conditions studied. A possible physical explanation is the solidification of the polymer solution taking place simultaneously with the emulsification. The importance of the solidification increases rapidly with the decrease in the droplet size, and at a given point it becomes a predominant factor. This is understandable keeping in mind the tremendous increase in the area of contact between the two mixing phases. For example, the decrease in the emulsion drop radius from 5 to 1 μm causes a factor of 25 increase in the interfacial area. Since the rate of GBL attrition depends on the number of molecules transferred through a unit of area, the rate at which droplets solidify will also increase by the same factor. Further deformation and bursting of the elongated emulsion drops do not take place even if the shear is increased because the polymer is already in a "solid" state. Thus, the process of decreasing the rod size by higher shear stress rapidly becomes inefficient and impractical below a certain range of sizes.

Table 2. Summary of Results on the Influence of the Polymer Concentration and Viscosity Ratio, *p*, on SU-8 Rod Formation in Two Different Media, Glycerol (High Viscosity) and Its Mixture with Ethylene Glycol (of Lower Viscosity)

	glycerol		glycerol/ethylene glycol (50:50, v/v)	
[SU-8], wt %	$p = \mu_1/\mu_0$	rod formation	$p = \mu_1/\mu_0$	rod formation
6	0.006	no	0.054	no
10.9	0.007	no	0.07	no
16.4	0.01	no	0.093	no
22.2	0.013	no	0.126	some rods
31	0.02	no	0.2	rods
38.7	0.04	some rods	0.359	rods
48.2	0.2	rods	1.94	rods
53.7	0.53	rods	5.15	rods
63	3.47	rods	33.9	rods

The minimal value of *a* suggests a limit to the minimal dimensions of the rods formed. Rods with an average length shorter than about 15 μm were not observed in the experiments with the concrete polymer/solvent/medium system studied (Figure 5). However, the subtle balance between the rates of emulsification and solidification should allow a certain degree of freedom in further decrease of the rod sizes. Reducing the rate of attrition of the primary polymer solvent (GBL) and decreasing the polymer concentration might allow emulsification into smaller emulsion drops and obtainment of rods of smaller sizes.

4.4. Effect of the Polymer Concentration and Viscosity Ratio, *p*, on Microrod Formation. The previous sections demonstrate that the presence of polymer and the resulting droplet solidification are important in the later stages of the process. The change in polymer concentration affects the viscosity of the emulsified phase and the rate of solvent attrition. More viscous droplets will retain their deformed shape without bursting into smaller ones while the solvent is redistributing to the surrounding medium. The SU-8 rod formation was studied with two different dispersion media, pure glycerol and its 50:50, v/v, mixture with ethylene glycol. For each case $p = \mu_1/\mu_0$ was affected through the viscosity of the polymer solution, μ_1. The viscosity of the SU-8 solution dropped dramatically upon dilution with GBL, reaching a plateau value at about 15−20 wt % SU-8. The range of the shear stress applied in each system was varied between 97 and 388 Pa for glycerin and between 10 and 99 Pa for the glycerol/ethylene glycol mixture. The SU-8 concentrations and viscosity ratios and the results of qualitative observations of whether rods were formed from the solutions at any shear stress are summarized in Table 2.

The data in Table 2 point out that, for each dispersion medium studied, formation of rodlike particles occurred only above a given value of polymer concentration and viscosity ratio. Rods were not formed at small polymer concentrations corresponding to low *p* (low viscosity of the SU-8 solution). Instead, spherical, or a mixture of spherical, disklike, and flocculated, particles were obtained (Figure 8a) at $p < 0.04$ for glycerol and at $p <$

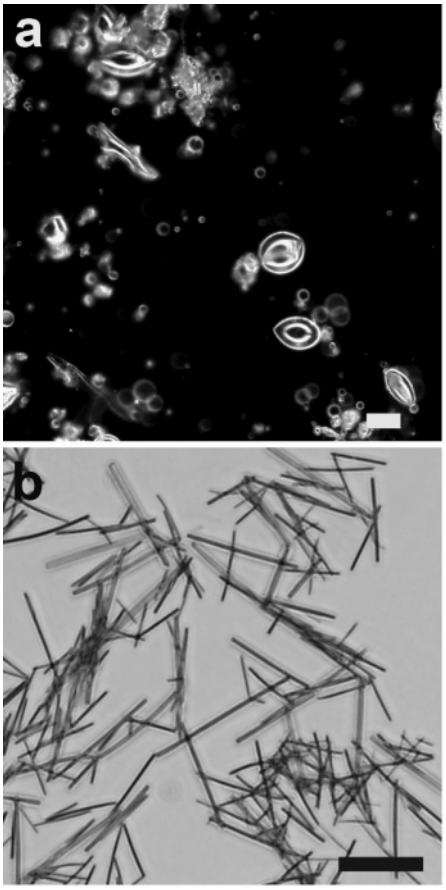

Figure 8. Effect of the polymer concentration and viscosity ratio, *p*, on the microrod formation process: (a) optical microscopy image of polymer drops solidified when the initial SU-8 solution is emulsified at a viscosity ratio of 0.02; (b) well-shaped rodlike particles at a high viscosity ratio of 0.2. The dispersion medium is glycerin, and the initial concentration of SU-8 is 31 wt %. The scale bars are 50 μm.

0.13 for the glycerol/ethylene glycol mixture. At higher polymer concentrations, nicely shaped cylindrical particles were formed (Figure 8b).

The observed strong influence of the polymer concentration on the process outcome has a few possible origins. First, the viscosity of the polymer solution is lowered by increasing the GBL concentration. Second, as GBL is soluble in the outside medium, this leads to a decrease of the interfacial tension and increased mass transfer of GBL molecules through the interface. Smaller values of γ increase the capillary number, and therefore promote droplet deformation and breakup. However, the interfacial area increases tremendously with the decreasing droplet size, which leads to a substantial increase in the mass transfer. The drops solidify before they are deformed into cylinders, resulting in spherical or only slightly deformed particles.

We proved that the solidification during droplet elongation under shear is a critical component of rod formation. If the polymer drops were not solidified while deformed, they restored their spherical shape when the shear was removed. Experiments performed with a photopolymer (HDDA) that does not solidify resulted in a polymer emulsion that produced spherical polymer particles after UV cross-linking. Additional evidence for the importance of the solidification was obtained by attempting to prepare SU-8 rods using a dispersion medium that contained some GBL, acetone, or another good solvent for SU-8. When the concentration of GBL in the dispersion medium was high enough to ensure comparable values of its chemical potential in both the SU-8 solution and the outside medium, the emulsion drops restored their spherical shape after the shear stress was removed (see the Supporting Information). Therefore, the effect of the polymer concentration on the rod formation process should also be examined from the viewpoint of the rate of solvent attrition.

The rate of solidification has to be neither very high nor very low. Too rapid solvent attrition will not allow enough time for uniform deformation to take place, while too slow solidification may worsen particle quality through droplet coalescence. Some insights about the role of the rate of GBL attrition may be derived from the comparison between the results for series I and II in Table 2. The viscosity of pure glycerol (1.040 Pa s) is about 10 times larger than that of its mixture with ethylene glycol (0.1062 Pa s). A larger μ_0 means smaller values for the diffusion coefficient of the transferring GBL molecules inside the dispersion medium. Thus, the solidification would be slower for a more viscous medium, and rodlike particles should be formed at lower values of the viscosity ratios. This is in agreement with the experimental observations that rods are formed at much higher values of *p* in the mixture than in the pure glycerol.

4.5. Fabrication of Composite Polymer−Nanoparticle Rods. The previous subsections demonstrate how we can control the length and diameter of the rods. The method also allows synthesis of rodlike particles of other polymers or their mixtures. Rods comprising two or more polymers can be obtained if all the polymers are dissolved in the initial solvent.[26] Another interesting modification of the method is the preparation of composite microrods containing nano- and microparticles. The only condition required is that the particles have to be dispersed in the original polymer solution. When a solution of SU-8 in GBL containing dispersed solid particles is subsequently sheared in a viscous medium, polymer rods containing embedded particles are formed. The presence of the solid particles, especially at low volume fractions (10−20% of the polymer volume), does not seem to alter noticeably the mechanism of emulsification and droplet deformation. The solid particles remain irreversibly trapped inside the solidified polymer during the rapid formation of the rods. These particles can modify the mechanical properties of the polymer rods, and can impart additional functionality.

The first demonstration of the formation of composite rods was done using a dispersion of silica spheres in 50% SU-8 in GLB. The dry silica powder was initially dispersed in GLB and then mixed with a concentrated solution of SU-8 in GLB. The process of rod formation and the characteristic dimensions of the obtained particles were very similar to those in the case of a pure SU-8 solution. The silica particles embedded in the rods appear as darker spots in Figure 9a. We also demonstrated preparation of SU-8 microrods with embedded superparamagnetic particles. The magnetic particles were introduced into the polymer solution from commercial superparamagnetic particles as described in the Experimental Section. Neither of the samples studied showed the presence of free magnetic particles in the dispersion phase, confirming that all of the initially added solid particles remained trapped inside the solidified polymer. An optical micrograph of "magnetic" rods is presented in Figure 9b. The incorporation of magnetic particles in the polymer leads to the formation of rods that readily respond to an external magnetic field.[40] The whole range of potentially useful properties of the new colloid material is reviewed in the next subsection.

4.6. Properties and Applications of Polymer Microrod Suspensions. Suspensions of rodlike particles have interesting properties and important applications. In this section we overview

(40) Wege, H.; Alargova, R. G.; Velev, O. D.; Paunov, V. N. *Adv. Funct. Mater*., submitted for publication.

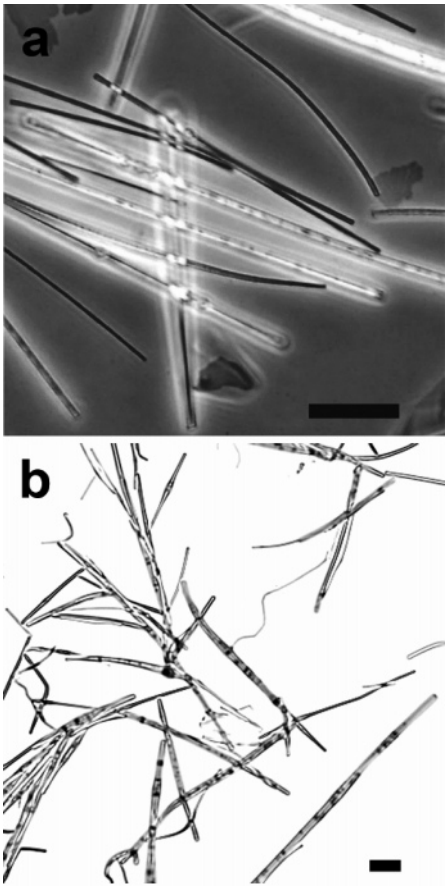

Figure 9. Examples of composite rods formed by dispersing inorganic particles in the initial SU-8 solution, which remain trapped within the microrods: (a) rods containing silica spheres and (b) rods containing paramagnetic particles. The scale bars are 10 μm.

and discuss briefly some of the bulk and interfacial properties of the microrod suspensions. A collection of experimental images illustrating these properties is presented in Figure 10.

Organization into Liquid-Crystal-like Phases. Due to the strong excluded volume interactions between cylinders, the effective volume fraction of rods is much higher than that of spheres with the same volume. The concentration at which rods start forming structures in the bulk of suspensions is much lower than for spheres. The SU-8 microrods readily organized into liquid-crystal-like phases during sedimentation or drying. The particles may also align parallel to each other by attractive lateral interactions. Hydrophobic rods tend to aggregate reversibly in the bulk, forming clusters in which all particles are aligned in one direction. The quality of the liquid-crystalline phases obtained may be improved by tuning the surface properties of the particles.

We found that SU-8 rods dispersed in dodecane formed larger nematic-like domains than in water or other solvents. This can be explained by the smaller van der Waals and hydrophobic attraction between rods in dodecane (compared to water), which allowed better realignment. Domains of microrods organized in nematic-like liquid-crystal phases were observed in drying droplets of dispersions containing more than 1−2 wt % particles (Figures 1d and 10a). Images taken with crossed polarizers show a certain degree of birefringence due to the presence of domains in which all particles lie in one direction (Figure 1d). Different domains are oriented in different directions due to the lack of long-range correlation during the nucleation process. Long-range directional orientation of the rods can be achieved by using magnetic and electric fields as explained in the next subsection.

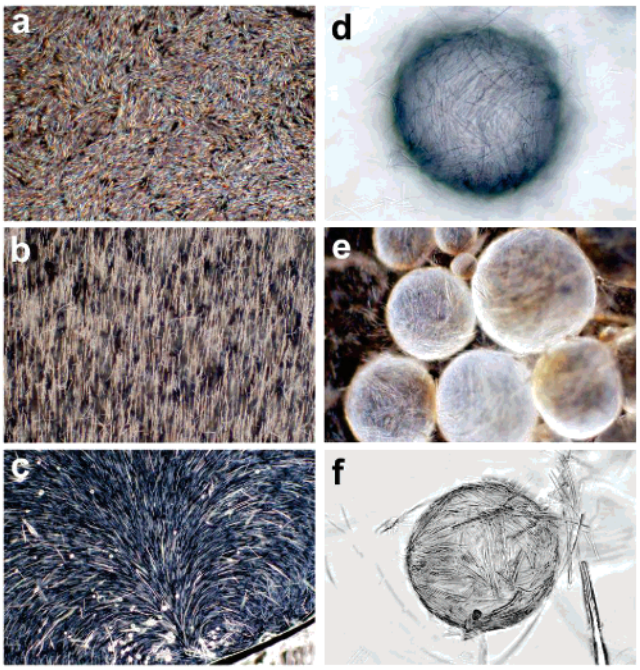

Figure 10. Examples of the alignment and stabilization properties of the polymer microrods synthesized by the methods discussed here: (a) aligned domains of microrods deposited by drying of a droplet of rod suspension in dodecane; (b) microrods containing magnetic particles in suspension aligned in an external magnetic field; (c) rods visualizing the convective flow near the liquid interface on the bottom; (d) rigid rod shell around an air bubble leading to the effect of foam superstablization described earlier;[27] (e) stable emulsion of decane droplets in water protected by rod shells; (f) colloidosome capsule of microrods mechanically connected by cross-linking.[29]

Alignment and Manipulation by External Fields. Previously we showed that long-range orientation of SU-8 microrods in the same direction can be induced by applying an external ac field.[26] The rods align in the direction of the field lines due to the dielectrophoretic torque.[41] The magnetic rods synthesized in this study allowed an even easier way of controlling the rod orientation by external magnets (Figure 10c).

Alignment in Liquid Flows. An alternative means to orient rapidly the polymer microrods parallel to each other was hydrodynamic flow. The parallel component of the drag force acting on a rod placed in shear hydrodynamic flow is much smaller than the perpendicular one. Any rodlike particle that does not point in the direction of the flow lines would experience a torque that will force it to align parallel with the flow. Even upon rocking by hand, the vials with SU-8 rod dispersions acquired a silverfish color, indicating some birefringence. The alignment of the microrods allows immediate visualization of flow lines on the microscale. Closer examination of the rod behavior in a flow using an imaging microscopy chamber containing microchannels 500−1000 μm in width at a flow rate of 5−100 μL/min revealed that all rods are oriented along the flow direction. The use of microrods for visualizing flow lines on the microscale may be an easier and more convenient alternative to conventional particle tracking techniques. The microrod suspensions only require a single snapshot, instead of recording a sequence of images and tracking digitally the position of many particles. An example of the visualization of liquid microcirculation due to Marangoni flow near an evaporating surface is shown in Figure 10c.

(41) Jones, T. B. *Electromechanics of Particles*; Cambridge University Press: Cambridge, U.K., 1995.

Stabilization of Foams, Emulsions, and Shell-like Capsules. We found earlier that the foams formed from rod suspensions have very high stability, largely exceeding the stability of foams containing conventional ionic surfactant.[27] The origin of this "superstabilization" effect is the formation of rigid shells of intertwined rods around the surfaces of the bubbles (Figure 10d), providing mechanical and steric stabilization of the films formed between the bubbles in contact.[27] Thus, superstabilization is largely a result of the strong adsorption of the microrods at the air−water interface, which in turn occurs when the rod surfaces are partially hydrophobic. The degree of hydrophobicity of the rods depended on the effectiveness of the removal of surface-active molecules from the dispersion medium in which the rods have been synthesized. Multiple washing with deionized water increased the rod hydrophobicity, leading to a contact angle of ca. 84° at the air−water interface and ca. 114° at the tricaprylin−water interface (for experimental images of adsorbed rods, see the Supporting Information for ref 27). Such particles adsorb strongly on liquid−air and liquid−oil surfaces. Rod hydrophobicity could be tuned by adding small amounts of amphiphiles. The superstabilization effect[27] has been first demonstrated with foam bubbles (Figure 10d). Tests with the rods synthesized in the present study proved that the microrods can act as superstabilizers of emulsion droplets (Figure 10e). Notably the rods can be used for long-term stabilization of systems that are hard to protect with regular surfactants, such as emulsions of low-molecular-weight hydrocarbons (e.g., hexane) in water or water-in-oil emulsions. A detailed account of the emulsion stabilization with these particles will be presented elsewhere.[28] Another possible application of the rigid shells formed by microrods around emulsion droplets can be the fabrication of semipermeable capsules after the internal droplet is removed or replaced. Earlier research on such "supraparticle" or "colloidosome" capsules has demonstrated their potential in various drug delivery, pharmaceutical, or food applications.[42,43] We have demonstrated that the microrods can be used for making such rigid semipermeable colloidosome capsules around droplets containing agarose gel (Figure 10f).[29] Thus, microrods can not only substitute for regular surfactant in stabilizing various colloidal systems and products but also form the basis of new colloidal assemblies of advanced structure and functionality. One additional potential application that has not been explored in detail yet is the formation of long fibers when polymers of large molecular weight are used (as demonstrated by the polystyrene fibers shown in Figure 3). Such fibers can form the basis of nonwoven textiles, filters, and other porous materials. Presently, the major and intensely studied method for the formation of similar thin polymer fibers is electrospinning;[44−47] however, the scaleup capacity of this method is limited, and the cost of the product is relatively high. Longer microrods and fibers similar to the ones in Figure 3 may present a cost-effective alternative to polymer fiber materials made by electrospinning and other extrusion techniques. The microrods can also find applications as fillers in polyurethane and latex foams, substituting for presently used latex spheres and potentially modifying their mechanical properties.

5. Conclusions

The advent of nanoscience has spanned an interest in the synthesis of classes of particles with novel shape and functionality. Large progress has been made in the synthesis of various inorganic and metallic particles of rodlike and other shapes. The achievements in the area of synthesis of polymer rods and other polymer particles of complex shape are much more modest. The method for synthesis of polymer microrods reported in detail here is scalable and rapid, and thus can be of practical importance if the mechanisms and the controlling factors are understood. The concepts used in interpreting the data are based on earlier theories of shear-induced emulsification, deformation, and breakup of emulsion droplets. Even though the processes taking place in our system are much more complex than simple emulsification, the data can be explained reasonably well on the basis of these concepts. This allows robust multivariate control over the size, shape, and polydispersity of the particles fabricated. The development of principles for control and scaling up of the process for microrod formation can have important implications, due to the wide range of possible application of this colloidal material. The superstabilization of foams and emulsions and the formation of rigid capsules could be used in various products including, e.g., food dispersions, polyurethane and latex foams, and detergent and pharmaceutical formulations. We believe that the controlled large-scale formation of polymer particles with an asymmetric shape and new functionality has a significant potential and might be a subject of intense research in the future.

Acknowledgment. This study was supported by NER and CAREER grants from the National Science Foundation and by an EPSRC grant (U.K.). We are grateful to Devdutta Warhadpande for synthesizing some of the rod samples, to Brian Prevo and Daniel Kuncicky for help with SEM, and to Angelica Sanchez and Saad Khan for assistance with the rheometer experiments.

Supporting Information Available: Data for SU-8 rods prepared by shaking and stirring and in a high-shear coaxial rheometer and summary of results for rod formation in various dispersion media. This material is available free of charge via the Internet at http://pubs.acs.org.

LA051825V

(42) Velev, O. D.; Furusawa, K.; Nagayama, K. *Langmuir* **1996**, *12*, 2374.
(43) Dinsmore, A. D.; Mink, F.; Hsu, M. G.; Nikolades, M. G.; Marques, M.; Bausch, A. R.; Weitz, D. A. *Science* **2002**, *298*, 1006.
(44) Doshi, J.; Reneker, D. H. *J. Electrost.* **1995**, *35*, 151.
(45) Dror, Y.; Salalha, W.; Khalfin, R. L.; Cohen, Y.; Yarin, A. L.; Zussman, E. *Langmuir* **2003**, *19*, 7012.
(46) Theron, A.; Zussman, E.; Yarin, A. L. *Nanotechnology* **2001**, *12*, 384.
(47) Li, D.; Xia, Y. N. *Adv. Mater.* **2004**, *16*, 1151.